NUCL SCI TECH (2016) 27:142
DOI 10.1007/s41365-016-0134-2

Preparation and biodistribution assessment of ^{68}Ga-DKFZ-PSMA-617 for PET prostate cancer imaging

Mehdi Sharifi[1] · Hassan Yousefnia[1] · Samaneh Zolghadri[1] · Ali Bahrami-Samani[1] · Mojdeh Naderi[2] · Amir Reza Jalilian[1] · Parham Geramifar[3] · Davood Beiki[3]

Received: 19 October 2015 / Revised: 14 January 2016 / Accepted: 15 January 2016 / Published online: 18 October 2016

Abstract Prostate-specific membrane antigen (PSMA) is a useful target for diagnostic and therapeutic applications, and it is demonstrated that ^{68}Ga in conjugation with DKFZ-PSMA-617 is better than ^{68}Ga-PSMA-1 in biodistribution data after 1 h, but more preclinical data are still required. In this paper, we presented the additional preclinical data for ^{68}Ga-DKFZ-PSMA-617 and relevant aspects of its production. ^{68}Ga was obtained from the SnO_2-based ^{68}Ge/^{68}Ga generator. Optimum conditions (pH, temperature, time and ligand concentration) for ^{68}Ga-DKFZ-PSMA-617 preparation were studied. Radiochemical purity of the radiolabeled compound was determined by HPLC and RTLC. After stability assessments, the complex was intravenously injected into rats. HPLC and ITLC characterizations indicated that the radiopharmaceutical could be prepared with radiochemical purity of >96 % and specific activity of 308.3 TBq/mmol at the optimized conditions (pH of 3.5–4, ligand amount of 2.4 nmol, temperature of 90–95 °C and reaction time of 10 min). Also, the biodistribution data showed no undesirable uptake in nontarget organs at any interval after injection. In fact, the activity is cleaned from blood and excreted rapidly via the kidneys. Generally, this compound can be considered as a well-established PET imaging agent.

Keywords ^{68}Ga · PSMA · Biodistribution · Imaging

1 Introduction

Prostate cancer (PC), as the most common men cancers in Europe, is still one of the outstanding reasons among cancer deaths [1]. However, the 5-year survival rate for an early detection of localized gland prostate cancers is almost 100 %, the cancer spread beyond the prostate leads to significant falling of the survival rates [2], and unfortunately mortality from metastasizing prostate cancer is still high [1]. Nowadays, an early detection of the metastatic lesions has significant impact on the clinical staging and therapy management of the patients [3, 4].

The prostate-specific membrane antigen (PSMA) also called glutamate carboxypeptidase II (GCP II) is expressed by almost all prostate cancers and gained the highest clinical impact in the past years. Due to the high-quality PET imaging of prostate cancer, PSMA has been known as an ideal target for this purpose [5–7] and some PSMA inhibitors in labeling with ^{68}Ga [8–11] and ^{123}I [12] have shown promising results in first human studies.

Studies on the recently prepared Glu-NH-CO–NH-Lys-(Ahx)-[^{68}Ga(HBED-CC)] (^{68}Ga-PSMA-11) as a ^{68}Ga-labeled PSMA ligand showed the ability of tracer for high-contrast detection of PC relapses and metastases [8, 13]. Also, the comparison of this PET imaging agent with ^{18}F-fluoromethylcholine PET/CT as the choline-based PET/CT demonstrated the detection of lesions with improved contrast, especially at low PSA levels [9].

✉ Hassan Yousefnia
hyousefnia@aeoi.org.ir

[1] Nuclear Science and Technology Research Institute (NSTRI), Tehran 14395-836, Iran

[2] Department of Chemistry, University of Zanjan, Zanjan 4537138791, Iran

[3] Research Center for Nuclear Medicine, Shariati Hospital, Tehran University of Medical Sciences, Tehran 1411713135, Iran

Besides the slightly modified chemical structure of the molecules synthesized for binding to PSMA, these molecules differ mainly in the selection of the chelator for the complexation of the desired radionuclide [14–16]. 1,4,7,10-Tetraazacyclododecane-*N*,*N*′,*N*″,*N*‴-tetraacetic acid (DOTA) is the mostly used chelator for the complexation of radiometals such as ^{68}Ga, ^{177}Lu and ^{166}Ho, especially to small molecules [17–19] either for diagnostic or for therapeutic applications. 2-[3-(1-Carboxy-5-{3-naphthalen-2-yl-2-[(4-{[2-(4,7,10-tris-carboxymethyl-1,4,7,10-tetraaza-cyclododec-1-yl)-acetylamino]-methyl}-cyclohexanecarbonyl)-amino]-propionylamino}-pentyl)-ureido]-pentanedioic acid (DKFZ-PSMA-617) as the recently DOTA-based synthesized PSMA (Fig. 1) labeled with ^{177}Lu has indicated a high potential to improve the clinical management of advanced PC in its first human study [20–22].

^{68}Ga is an excellent positron-emitting radioisotope suitable for clinical PET imaging. Having physical characteristics of positron emission (89 %), low abundance of 1077 keV photon emission (3.22 %) and relatively short half-life ($t_{½}$ = 67.71 min) [22], it permits PET applications of the ^{68}Ga-radiopharmaceuticals, with an acceptable radiation dose to the patient [23]. With the extension of PET and the construction of ^{68}Ge/^{68}Ga generators with suitable eluates for labeling, the use of ^{68}Ga has arisen recently [19].

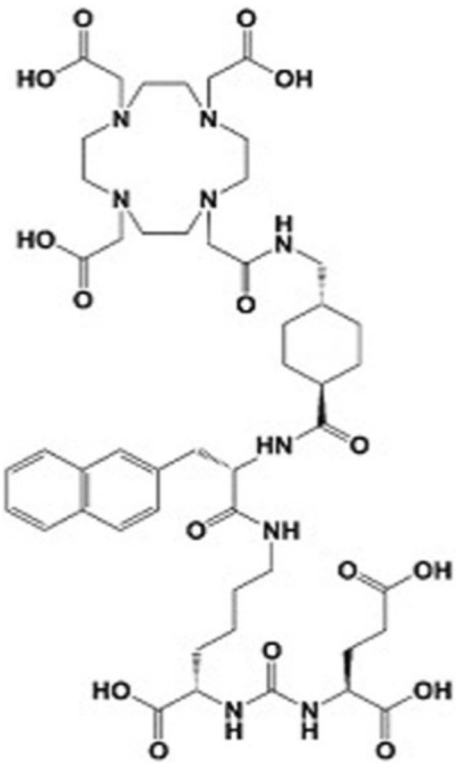

Fig. 1 Chemical structure of DKFZ-PSMA-617 [21]

The clinical impact of the PSMA PET tracers is growing very fast. Recently, ^{68}Ga-DKFZ-PSMA-617 was designed and its first individual clinical experience showed comparable results with ^{68}Ga-PSMA-11 [21], but it is better than ^{68}Ga-PSMA-11 in the uptake ratio of tumor to blood and muscle after 1 h [21]. However, more preclinical data on its biodistribution in different organs and at specified times after injection are required for performance evaluation of this new compound before clinical usage.

In this paper, we present the additional preclinical data of ^{68}Ga-DKFZ-PSMA-617 and relevant aspects of its production. The ^{68}Ga-DKFZ-PSMA-617 was prepared at the optimized conditions (pH, temperature, ligand concentration and reaction time), and the appropriate systems for HPLC and RTLC analysis were introduced. The biodistribution data of the radiolabeled compound were investigated in male Syrian rats at given intervals from 15 min to 2 h after injection by killing and PET imaging. $^{68}GaCl_3$ was injected to the same type rats for biodistribution comparison of the organ uptake of the radiolabeled compound.

2 Experimental section

A prototype 40-mCi ^{68}Ge/^{68}Ga generator, developed at Pars Isotope Co. (Tehran, Iran), was used in this study. ^{68}Ge/^{68}Ga generator was eluted with supra-pure HCl (0.6 mM, 5 mL) in 0.5-mL fractions. Three fractions with the highest $^{68}GaCl_3$ activity were used for labeling purposes. DKFZ-PSMA-617 was provided from ABX (Radeberg, Germany). The other chemical reagents were from Sigma-Aldrich Chemical Co. (UK). Whatman No. 2 paper was from Whatman (UK). Radiochromatography was performed by Whatman paper using a thin-layer chromatography scanner, Bioscan AR2000 (Paris, France). Activities of the samples were measured by a p-type coaxial high-purity germanium detector (HPGe, EGPC 80-200R) coupled with a multichannel analyzer. Calculations were based on the 511-keV peak for ^{68}Ga. All values were expressed as mean ± SD, and the data were compared using Student's *T* test. Statistical significance was defined as $P < 0.05$. Animal studies were performed in accordance with the United Kingdom Biological Council's Guidelines on the Use of Living Animals in Scientific Investigations, second edition.

2.1 Elution of ^{68}Ge/^{68}Ga generator

For selecting appropriate eluent, the generator was eluted by 5 mL HCl with different concentrations from 0.1 to 1.0 M and the activity of the eluted ^{68}Ga was measured utilizing HPGe detector at each time. Also, in order to

optimize the minimum required volume for the elution of ^{68}Ga with the maximum yield and radioactive concentration, the generator was eluted with the equal volume of HCl and the activity of each fraction containing 0.5 mL of the eluate was measured.

2.2 Quality control of the eluted ^{68}Ga

The radionuclidic purity of the product was investigated by gamma spectrometry. This step was carried out utilizing an HPGe detector coupled to a Canberra^{TM} multichannel analyzer for 1000 s. Breakthrough was measured by counting the same sample at 48 h after the first test for the detection of a small amount of ^{68}Ge in the sample.

The chemical purity control of the sample was carried out by the ICP-OES method, to ensure that concentrations of tin (from generator material), iron (from the sealing parts and acid impurities), zinc (as the decay product) and gallium (as the target material) were acceptable regarding the internationally accepted limits.

Radiochemical purity of the eluted ^{68}Ga was studied using ITLC. ITLC chromatograms of $^{68}GaCl_3$ solution were performed in 10 % ammonium acetate/methanol on silica gel sheets and in 10 mM DTPA solution (pH = 4) on Whatman No. 2 paper.

2.3 Radiolabeling of DKFZ-PSMA-617 with $^{68}GaCl_3$

A stock solution of DKFZ-PSMA-617 in concentration of 1 μg/μL in distilled water was prepared. The first fraction of the eluted ^{68}Ga was put away, and the next three fractions including 1.5 mL of $^{68}GaCl_3$ (approximately 925 MBq) were used for radiolabeling. Certain amount of DKFZ-PSMA-617 was added to the vial containing $^{68}GaCl_3$, and the pH of the reaction mixture was adjusted utilizing HEPES (1 M in H_2O). In order to obtain the optimized conditions, several experiments were performed by changing the ligand concentration, pH, temperature and incubation time.

Then, 8 mL of water was added to the final solution and the mixture was passed through a C_{18} Sep-Pak column which preconditioned with 5 mL ethanol, 10 mL water and 10 mL air, respectively. The column was then washed with 0.5 mL ethanol and 1 mL of 0.9 % NaCl. The volume of the final solution was adjusted to 5 mL by 0.9 % NaCl before injection.

2.4 Quality control of the radiolabeled complex

Radiochemical purity of the radiolabeled complex was checked using both HPLC and ITLC methods. Paper chromatography was carried out using Whatman No. 2 paper and 0.9 % NaCl and 0.1 M sodium citrate as the mobile phases.

HPLC was performed on the final preparation utilizing a C_{18}ODS column with the dimensions of 100 mm × 4.6 mm and 5 μm particle size. Gradient elution was applied with the following parameters: A = water + 1 % TFA, B = acetonitrile, flow rate: 2.6 mL/min, 100 % A:0 % B for 3 min, 50 % A:50 % B for 7 min, 0 % A:100 % B for 5 min.

2.5 Stability tests

In order to check the stability in the final product, a sample of ^{68}Ga-DKFZ-PSMA-617 (37 MBq) was kept at room temperature for up to 2 h while being checked by ITLC at the specified intervals.

Also, for the stability assessment of ^{68}Ga-DKFZ-PSMA-617 in human serum, 11.1 MBq of the final solution (50 μL) was added to the 300 μL of the freshly prepared serum and kept at 37 °C for 2 h. Every 30 min, trichloroacetic acid (10 %, 100 μL) was added to a portion of the mixture (50 μL), and the mixture was centrifuged at 3000 rpm for 5 min followed by decanting the supernatant from the debris. The stability was determined by performing frequent ITLC analysis of the supernatant using the above-mentioned ITLC system.

2.6 Biodistribution of $^{68}GaCl_3$ and the radiolabeled complex in Syrian rats

The 100 μL of final ^{68}Ga-DKFZ-PSMA-617 solution with approximately 5.55 MBq radioactivity was injected intravenously into male Syrian rats through their tail vein. Also, for better comparison, biodistribution of $^{68}GaCl_3$ in 0.9 % normal saline (pH = 7) was investigated followed by intravenous administration of 100 μL of the solution (5.55 MBq). The total amount of radioactivity injected into each animal was measured by counting the 1-mL syringe before and after injection in a dose calibrator with fixed geometry. The biodistribution of the solutions among tissues was determined by killing of four rats for each selected intervals (15, 30, 60 and 120 min) after injection using the animal care protocols.

Blood samples were taken immediately after killing. The tissues were weighed and rinsed with normal saline, and their activities were determined with a p-type coaxial HPGe detector coupled with a multichannel analyzer.

The percentage of injected dose per gram (%ID/g) for different organs was calculated by dividing the activity amount of each tissue (A) to the decay-corrected injected activity and the mass of each organ. All values were expressed as mean ± SD, and the data were compared using Student's T test.

2.7 Imaging studies

PET/CT imaging was performed with a PET/CT scanner (Biograph 6 TrueX; Siemens Medical Solutions). Static PET images were acquired for 5 min with three sets of emission images in 2 h after ^{68}Ga-DKFZ-PSMA-617 injection in the rats. In addition, PET emission scans were preceded by CT scans performed for anatomical reference and attenuation correction (spatial resolution 1.25 mm, 80 kV, 150 mA) with a total CT scanning time of 20 s. Reconstruction was performed using the iterative algorithm with attenuation correction. The reconstruction settings were 4 iterations and 21 subsets to a 256 × 256 matrix, with a post-filtering of 2 mm. Transmission data were reconstructed into a matrix of equal size by means of filtered back-projection, yielding a coregistered image set.

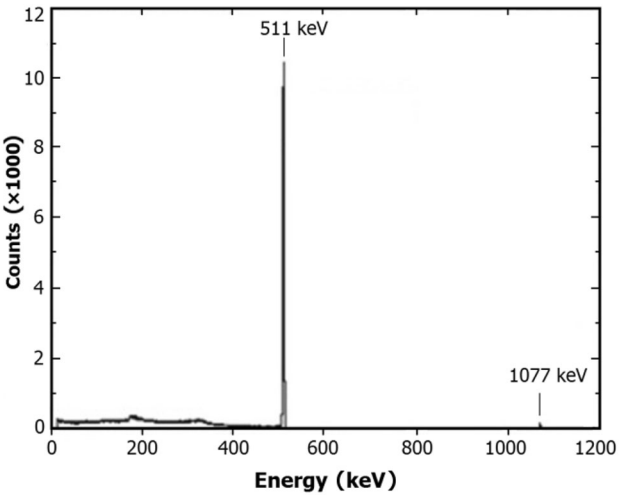

Fig. 2 Gamma spectrum of eluted $^{68}GaCl_3$

3 Results and discussion

3.1 Elution of ^{68}Ge/^{68}Ga generator

While the generator was eluted by 5 mL HCl with different concentrations of 0.1–1.0 M, activity of the eluted ^{68}Ga increased with the increment of HCl concentration. However, these data indicate higher elution yield for 1.0 M HCl, and 0.6 M HCl was determined as the more suitable solvent for radiolabeling purposes.

The generator was eluted with the equal volumes of 0.6 M HCl. The second, third and fourth fractions showed the maximum activities (>1110 MBq), and therefore, these fractions were used for radiolabeling purpose.

3.2 Quality control of the eluted ^{68}Ga

Radionuclidic control showed the presence of 511- and 1077-keV peaks, all originating from ^{68}Ga. The radionuclidic purity was higher than 99.9 %. Also, the calculations for Ge breakthrough demonstrated the ^{68}Ge/^{68}Ga activity ratio of about 9×10^{-6} at the time of elution. The HPGe spectrum of the solution is presented in Fig. 2.

The concentrations (in part per million) of tin (from generator material), iron (from the sealing parts and acid impurities), zinc (as the decay product) and gallium (as the target material) were 0.220, 0.230, 0.135 and <0.1, respectively. This chemical purity is crucial and usually suffices for the procedure.

The radiochemical purity of the $^{68}GaCl_3$ solution was checked in two solvent systems. In 10 mM DTPA solution, free $^{68}Ga^{3+}$ is coordinated with a more lipophilic moiety as $^{68}Ga(DTPA)^{2-}$ and migrates to a higher R_f. On the other hand, in a 10 % ammonium acetate/methanol mixture (1:1), $^{68}Ga^{3+}$ would remain at the origin, while any other ionic cation of $^{68}Ga^{3+}$ would migrate to higher R_f which was not observed here (Fig. 3).

3.3 Radiolabeling of DKFZ-PSMA-617 with $^{68}GaCl_3$

In order to obtain the maximum complexation yield, experiments were performed by varying the reaction parameters of ligand concentration, pH, temperature and reaction time. The effect of pH on complexation yield was studied at pH 3–5 of the reaction mixture using HEPES. As shown in Fig. 4a, the results indicate that the optimum pH for radiolabeling is 3.5–4.

The effect of the ligand amount on the radiochemical yield is shown in Fig. 4b. Even at very low concentration of the ligand (2.5 μg, 2.4 nmol), the high radiochemical purity can be achievable.

The effects of temperature and reaction time on radiochemical yield are given in Table 1. While the temperature of 90–95 °C is required, the experiments show that 10 min is sufficient for radiolabeling.

Totally, ^{68}Ga-DKFZ-PSMA-617 was prepared with the complexation yield of higher than 96 % and specific activity of 308.3 MBq/nmol at the optimized conditions which is about 2 times greater than the previous reported literature (140 MBq/nmol) [23].

3.4 Quality control of the radiolabeled complex

Radiochemical purity of the radiolabeled complex was checked using HPLC and ITLC. HPLC analysis demonstrated that the fast eluting compound was hydrophilic $^{68}GaCl_3$ cation (1.3 min), while ^{68}Ga-DKFZ-PSMA-617

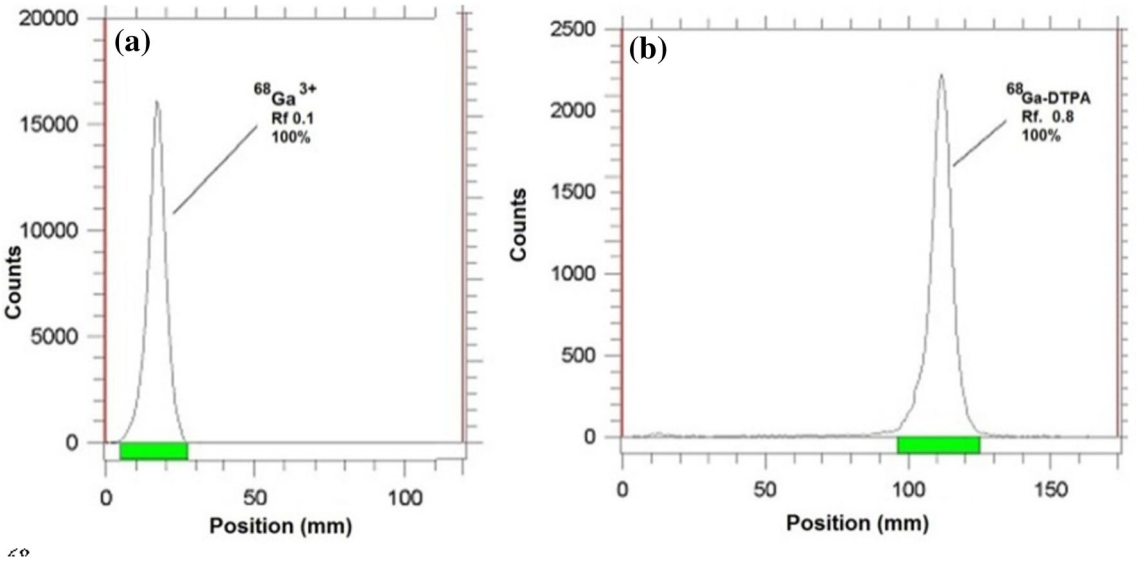

Fig. 3 ITLC chromatogram of $^{68}GaCl_3$ solution in (**a**) acetate/methanol 10 % ammonium (1:1) and (**b**) DTPA (pH.5) using Whatman No. 2

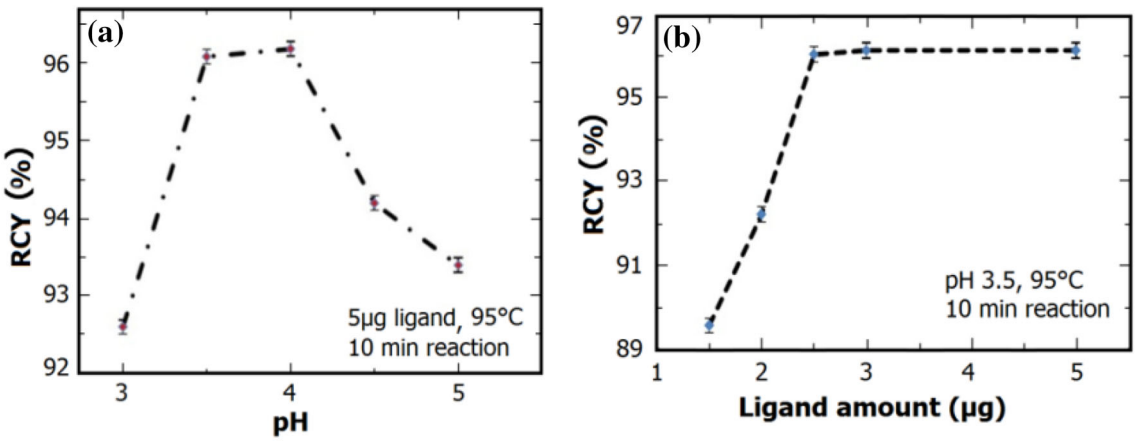

Fig. 4 Effects of pH (**a**) and ligand amount (**b**) on radiochemical yield. *Error bars* represent one standard error above and below the mean

Table 1 Effects of temperature and reaction time on radiochemical yield (%)

Temperature/°C (2.5 µg ligand, pH 3.5, 10 min reaction)				Reaction time/min (2.5 µg ligand, pH 3.5, 95 °C)			
50	70	85	95	5	10	20	30
32.4 ± 1.0	65.3 ± 0.9	88.6 ± 0.4	96.1 ± 0.7	92.6 ± 0.3	96.1 ± 0.6	96.0 ± 0.5	96.3 ± 0.8

with high molecular weight was eluted after 4.5 min (Fig. 5a). HPLC chromatogram showed the radiochemical purity of more than 96 %.

ITLC was applied for detecting the radiolabeled compound from the free gallium cation. In both 0.1 M sodium citrate and 0.9 % NaCl as the mobile phases with Whatman No. 2 as the stationary phase, the radiolabeled compound remains at the origin, while free gallium cation migrates to higher R_f (Fig. 5b, c). ITLC chromatogram also proved the radiochemical purity of over 96 %.

3.5 Stability studies

The stability of ^{68}Ga-DKFZ-PSMA-617 was investigated at room temperature and in human serum at 37 °C. The radiochemical purity of the complex remained >96 %

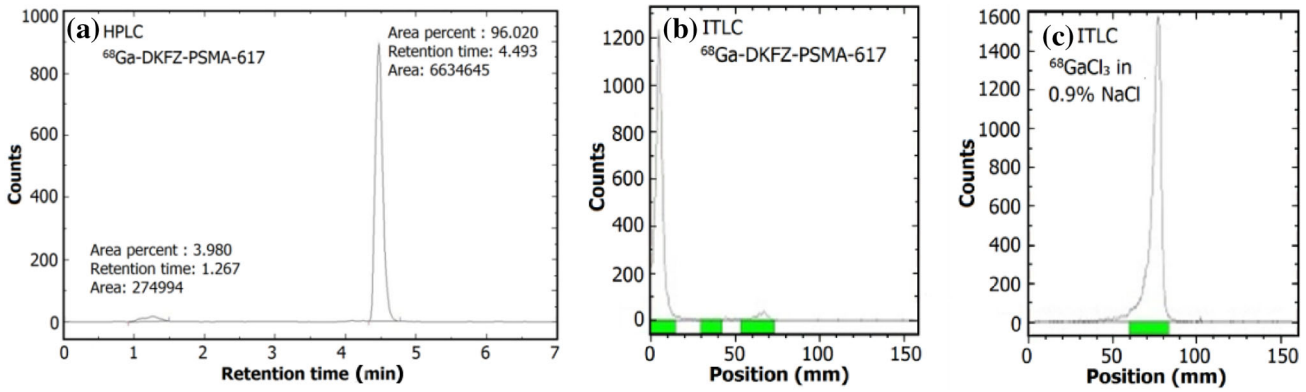

Fig. 5 HPLC (**a**) chromatogram of ^{68}Ga-DKFZ-PSMA-617 and ITLC chromatograms of ^{68}Ga-DKFZ-PSMA-617 (**b**) and $^{68}GaCl_3$ in 0.9 % NaCl (**c**) using Whatman No. 2

at room temperature and in freshly prepared human serum at 37 °C even after 120 min of preparation.

3.6 Biodistribution of $^{68}GaCl_3$ and the radiolabeled complex in Syrian rats

The tissue uptakes of $^{68}GaCl_3$ and the radiolabeled complex were calculated as the area percentage under the curve of the related photo peak per gram of tissue (% ID/g) (Tables 2 and 3). ^{68}Ga is mainly excreted from the gastrointestinal tract (GIT) with high blood contents due to the transferrin binding at early intervals. Also, the colon, bone and stomach activity contents are significant.

^{68}Ga-DKFZ-PSMA-617 demonstrated significant uptake in the kidney as the major route of excretion. The maximum uptake in the kidney occurred at 15 min post-injection while decreased with time. As expected, small accumulation was perceived in the prostate. The results indicated rapid clearance from blood. Approximately no activity was found after 30 min in blood samples. No significant accumulation was observed in the other organs.

The biodistribution pattern of ^{68}Ga-DKFZ-PSMA-617 is completely different from $^{68}GaCl_3$ (Fig. 6). Whereas the activity of $^{68}GaCl_3$ in blood decreases slightly with the time, the radiolabeled complex is cleared from blood rapidly (0.36 % after 30 min). The kidney is the major route of the excretion for the compound, while no considerable activity was accumulated in the kidney after $^{68}GaCl_3$ administration. Generally, accumulation of the complex in the most organs such as the intestine, liver,

Table 2 Percentage of injected dose per gram (%ID/g) at different minutes after intravenously injection of $^{68}GaCl_3$ (5.55 MBq) into Syrian rats

Organs	15 min	30 min	60 min	120 min
Blood	3.18 ± 0.17	2.98 ± 0.12	2.53 ± 0.11	2.44 ± 0.14
Kidney	0.70 ± 0.09	0.41 ± 0.10	1.42 ± 0.12	0.91 ± 0.08
Spleen	0.51 ± 0.09	0.70 ± 0.06	1.03 ± 0.10	1.43 ± 0.12
Stomach	0.41 ± 0.11	0.56 ± 0.07	1.21 ± 0.09	1.54 ± 0.14
Intestine	0.71 ± 0.06	0.82 ± 0.08	0.89 ± 0.05	0.61 ± 0.07
Liver	0.91 ± 0.02	1.50 ± 0.12	0.78 ± 0.08	0.60 ± 0.05
Bone	0.56 ± 0.06	0.91 ± 0.10	1.20 ± 0.11	1.05 ± 0.09

Table 3 Percentage of dose per gram (%ID/g) at different minutes in Syrian rats injected with 5.55 MBq ^{68}Ga-PSMA-DKFZ-PSMA-617

Organs	15 min	30 min	60 min	120 min	Organs	15 min	30 min	60 min	120 min
Blood	0.81 ± 0.05	0.36 ± 0.03	0.26 ± 0.01	0.18 ± 0.01	Skin	0.25 ± 0.03	0.15 ± 0.01	0.18 ± 0.01	0.06 ± 0.00
Herat	0.38 ± 0.02	0.14 ± 0.01	0.12 ± 0.01	0.00 ± 0.00	Bone	0.08 ± 0.00	0.03 ± 0.00	0.04 ± 0.00	0.07 ± 0.00
Kidney	23.74 ± 0.85	9.05 ± 0.54	3.63 ± 0.18	1.76 ± 0.10	Muscle	0.08 ± 0.00	0.04 ± 0.00	0.01 ± 0.00	0.04 ± 0.00
Spleen	0.13 ± 0.01	0.14 ± 0.02	0.10 ± 0.00	0.10 ± 0.01	Thyroid	0.31 ± 0.02	0.23 ± 0.01	0.45 ± 0.03	0.21 ± 0.04
Stomach	0.11 ± 0.02	0.09 ± 0.02	0.12 ± 0.01	0.13 ± 0.00	Adrenal	0.18 ± 0.02	0.46 ± 0.03	0.29 ± 0.03	0.47 ± 0.04
Intestine	0.14 ± 0.02	0.09 ± 0.01	0.15 ± 0.01	0.57 ± 0.04	Salivary gland	0.24 ± 0.03	0.20 ± 0.02	0.18 ± 0.01	0.24 ± 0.05
Lung	0.50 ± 0.06	0.30 ± 0.02	0.15 ± 0.01	0.10 ± 0.00	Pancreases	0.18 ± 0.01	0.14 ± 0.02	0.20 ± 0.01	0.10 ± 0.00
Liver	0.22 ± 0.04	0.14 ± 0.01	0.12 ± 0.02	0.08 ± 0.00	Prostate	0.86 ± 0.06	0.76 ± 0.05	0.99 ± 0.07	0.90 ± 0.04

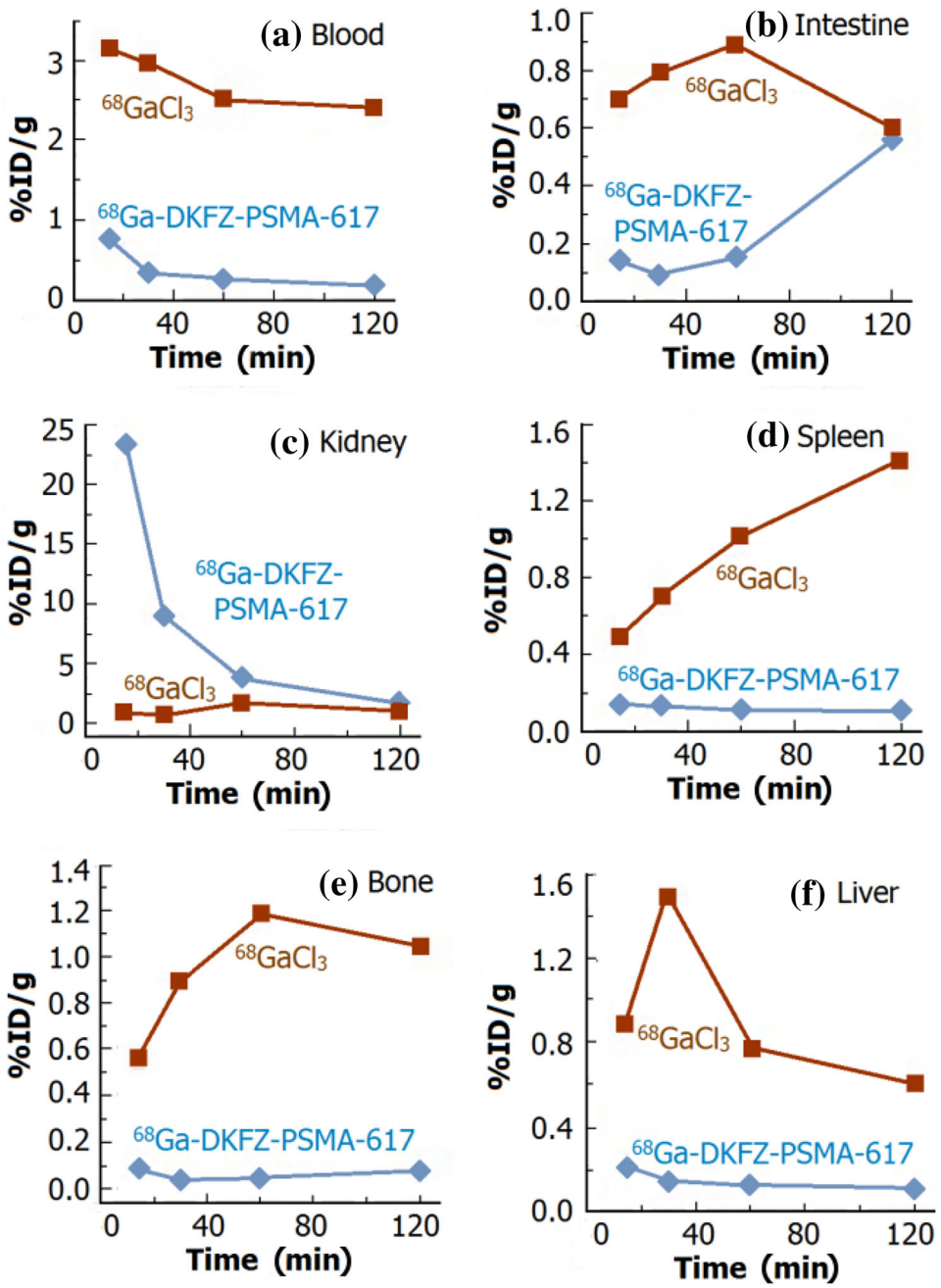

Fig. 6 Comparison of activities for $^{68}GaCl_3$ and ^{68}Ga-DKFZ-PSMA-617 in organs of normal Syrian rats

spleen and the bone is so much smaller than $^{68}GaCl_3$, which is a major advantage for this radiopharmaceutical.

Our study on ^{68}Ga-DKFZ-PSMA-617 indicates the benefit of its application over ^{68}Ga-PSMA-11 as the routinely used PSMA radiopharmaceutical, but the injected dose per gram of tissue is only presented at 1 h post-injection. With regard to the importance of activity distribution in nontarget organs, to avoid undesirable absorbed dose, biodistribution of this new radiopharmaceutical in different organs was studied from 15 min to 2 h post-injection. Significant accumulation was observed in the kidney, which is in accordance with the literatures [23]. Activity aggregation in the other organs is insignificant.

3.7 PET/CT imaging studies

Figure 7 shows typical PET/CT images acquired immediately and 30/60 min after ^{68}Ga-DKFZ-PSMA-617 injection in the normal Syrian rats. It can be seen that the only visible organs were the kidney and bladder. This confirms the imaging results in Ref. [23].

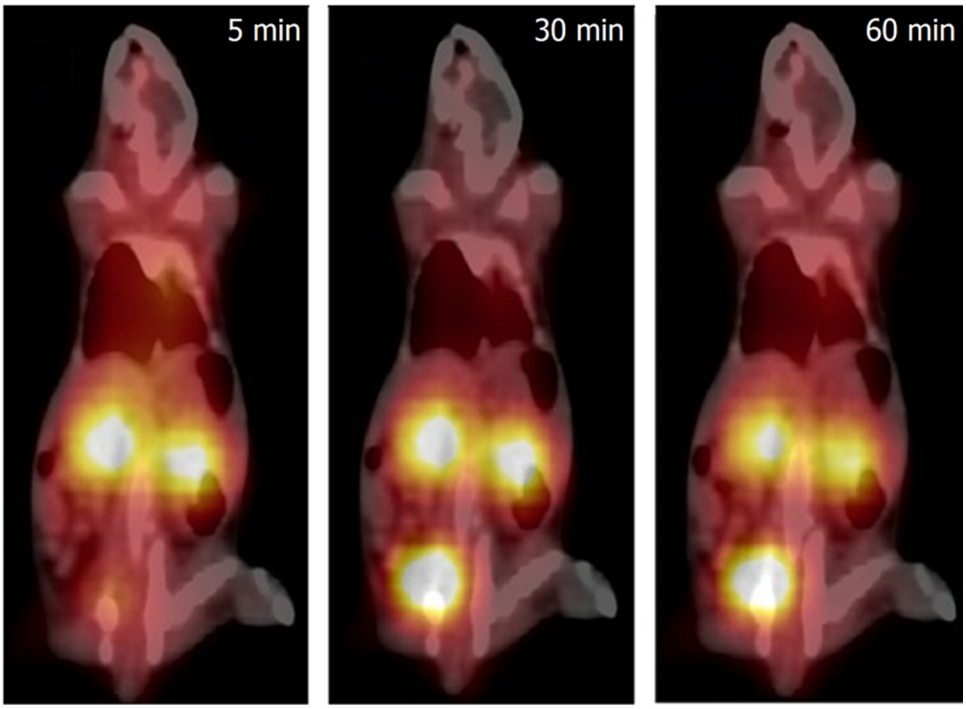

Fig. 7 PET/CT fused images of normal Syrian rats at different minutes after injection of 5.55 MBq ^{68}Ga-DKFZ-PSMA-617

4 Conclusion

In this work, ^{68}Ga was obtained from the SnO_2-based ^{68}Ge/^{68}Ga generator. The results of quality control analysis including radionuclidic, chemical and radiochemical purities indicated high purity of the eluted ^{68}Ga. The conditions for preparation of ^{68}Ga-DKFZ-PSMA-617 were optimized, with radiochemical purity of over 96 % and specific activity of 308.3 MBq/nmol in less than 10 min at 2.5 μg PSMA, pH 3.5–4 and 90–95 °C. We presented biodistribution of the ^{68}Ga-DKFZ-PSMA-617 complex in different intervals (15–120 min) in the organs of male Syrian rats after intravenous injection. Most of the injected activity was accumulated in the kidney which can be considered as the major route of the excretion. With regard to the insignificant amount of activity in other organs, this compound can be considered as a good agent for PET imaging applications.

References

1. R. Siegel, E. Ward, O. Brawley, A. Jemal, Cancer statistics, 2011: the impact of eliminating socioeconomic and racial disparities on premature cancer deaths. CA Cancer J. Clin. **61**, 212–236 (2011). doi:10.3322/caac.20121
2. American Cancer Society. Prostate cancer. http://seer.cancer.gov/statfacts/html/prost.html
3. G.L. Andriole, E.D. Crawford, R.L. Grubb 3rd et al., Mortality results from a randomized prostate-cancer screening trial. N. Engl. J. Med. **360**, 1310–1319 (2009). doi:10.1056/NEJMoa0810696
4. M. Beheshti, W. Langsteger, I. Fogelman, Prostate cancer: role of SPECT and PET in imaging bone metastases. Semin. Nucl. Med. **39**, 396–407 (2009). doi:10.1053/j.semnuclmed.2009.05.003
5. S.R. Banerjee, M. Pullambhatla, Y. Byun et al., ^{68}Ga-labeled inhibitors of prostate-specific membrane antigen (PSMA) for imaging prostate cancer. J. Med. Chem. **53**, 5333–5341 (2010). doi:10.1021/jm100623e
6. M. Eder, O. Neels, M. Müller et al., Novel preclinical and radiopharmaceutical aspects of [^{68}Ga]Ga-PSMA-HBED-CC: a new PET tracer for imaging of prostate cancer. Pharmaceuticals **7**, 779–796 (2014). doi:10.3390/ph7070779
7. A. Zaheer, S.Y. Cho, M.G. Pomper, New agents and techniques for imaging prostate cancer. J. Nucl. Med. **50**, 1387–1390 (2009). doi:10.2967/jnumed.109.061838
8. A. Afshar-Oromieh, A. Malcher, M. Eder et al., PET imaging with a [^{68}Ga]Gallium-labelled PSMA ligand for the diagnosis of prostate cancer: biodistribution in humans and first evaluation of tumour lesions. Eur. J. Nucl. Med. Mol. Imaging **40**, 486–495 (2013). doi:10.1007/s00259-012-2298-2
9. A. Afshar-Oromieh, C.M. Zechmann, A. Malcher et al., Comparison of PET imaging with a ^{68}Ga-labelled PSMA ligand and ^{18}F-choline-based PET/CT for the diagnosis of recurrent prostate cancer. Eur. J. Nucl. Med. Mol. Imaging **41**, 11–20 (2014). doi:10.1007/s00259-013-2525-5
10. A. Afshar-Oromieh, E. Avtzi, F.L. Giesel et al., The diagnostic value of PET/CT imaging with the (^{68})Ga-labelled PSMA ligand HBED-CC in the diagnosis of recurrent prostate cancer. Eur. J. Nucl. Med. Mol. Imaging **42**, 197–209 (2015). doi:10.1007/s00259-014-2949-6
11. M. Eiber, T. Maurer, M. Souvatzoglou et al., Evaluation of hybrid ^{68}Ga-PSMA ligand PET/CT in 248 patients with biochemical recurrence after radical prostatectomy. J. Nucl. Med. **56**, 668–674 (2015). doi:10.2967/jnumed.115.154153
12. J.A. Barrett, R.E. Coleman, S.J. Goldsmith et al., First-in-man evaluation of 2 high-affinity psma-avid small molecules for

imaging prostate cancer. J. Nucl. Med. **54**, 380–387 (2013). doi:10.2967/jnumed.112.111203
13. A. Afshar-Oromieh, U. Haberkorn, M. Eder et al., [^{68}Ga]Gallium-labelled PSMA ligand as superior PET tracer for the diagnosis of prostate cancer: comparison with ^{18}F-FECH. Eur. J. Nucl. Med. Mol. Imaging **39**, 1085–1086 (2012). doi:10.1007/s00259-012-2069-0
14. S.A. Kularatne, C. Venkatesh, H.K. Santhapuram et al., Synthesis and biological analysis of prostate-specific membrane antigen-targeted anticancer prodrugs. J. Med. Chem. **53**, 7767–7777 (2010). doi:10.1021/jm100729b
15. N. Malik, H.J. Machulla, C. Solbach et al., Radiosynthesis of a new psma targeting ligand ([^{18}f]fpy-dupa-pep). Appl. Radiat. Isot. **69**, 1014–1018 (2011). doi:10.1016/j.apradiso.2011.03.041
16. M. Eder, M. Schafer, U. Bauder-Wust et al., ^{68}Ga-complex lipophilicity and the targeting property of a urea-based PSMA inhibitor for PET imaging. Bioconjug. Chem. **23**, 688–697 (2012). doi:10.1021/bc200279b
17. W.A. Breeman, E. de Blois, H. Sze Chan et al., (^{68})Ga-labeled DOTA-peptides and (^{68})Ga-labeled radiopharmaceuticals for positron emission tomography: current status of research, clinical applications, and future perspectives. Semin. Nucl. Med. **41**, 314–321 (2011). doi:10.1053/j.semnuclmed.2011.02.001
18. H. Yousefnia, S. Zolghadri, H.R. Sadeghi et al., Preparation and biological assessment of ^{177}Lu-BPAMD as a high potential agent for bone pain palliation therapy: comparison with ^{177}Lu-EDTMP. J. Radioanal. Nucl. Chem. (2016). doi:10.1007/s10967-015-4225-z
19. H. Yousefnia, N. Amraei, M. Hosntalab et al., Preparation and biological evaluation of ^{166}Ho-BPAMD as a potential therapeutic bone-seeking agent. J. Radioanal. Nucl. Chem. **304**, 1285–1291 (2015). doi:10.1007/s10967-014-3924-1
20. C. Kratochwil, F.L. Giesel, M. Eder et al., [^{177}Lu]Lutetium-labelled PSMA ligand-induced remission in a patient with metastatic prostate cancer. Eur. J. Nucl. Med. Mol. Imaging **42**, 987–988 (2015)
21. Firestone RB, Shirley VS. Table of Isotopes. Wiley-VCH, 1998, 3168
22. M. Benešová, M. Schäfer, U. Bauder-Wüst et al., Preclinical evaluation of a tailor-made DOTA-conjugated PSMA inhibitor with optimized linker moiety for imaging and endoradiotherapy of prostate cancer. J. Nucl. Med. **56**, 914–920 (2015). doi:10.2967/jnumed.114.147413
23. S. Shanehsazzadeh, H. Yousefnia, A.R. Jalilian, Estimated human absorbed dose for ^{68}Ga-ECC based on mice data: comparison with ^{67}Ga-ECC. Ann. Nucl. Med. **29**, 475–481 (2015). doi:10.1007/s12149-015-0967-5